U. S. DEPARTMENT OF COMMERCE NATIONAL BUREAU OF STANDARDS

RESEARCH PAPER RP1474

Part of Journal of Research of the National Bureau of Standards, Volume 28, June 1942

PERFORATED COVER PLATES FOR STEEL COLUMNS: COMPRESSIVE PROPERTIES OF PLATES HAVING OVALOID PERFORATIONS AND A WIDTH-TO-THICKNESS RATIO OF 40

By Ambrose H. Stang and Martin Greenspan

ABSTRACT

Tests were made to determine the mechanical properties of perforated cover plates intended to be used as a substitute for lattice bars or batten plates in built-up box-type columns. Each test column was built up from one perforated plate and either two or four angles. Columns with unperforated plates were used as controls.

This paper gives the results of the tests on columns having plates of three different perforation spacings.

It was found that the perforated plates contributed to the strength, and especially to the stiffness, of the columns, and that the factor of stress concentration, due to the presence of the perforations, varied from 2 to 2.5 based on the gross area (1.8 to 2.1 based on the net area).

CONTENTS

I. INTRODUCTION

This paper is the second of a series dealing with the mechanical properties of perforated cover plates intended to be used as a substitute for lattice bars or batten plates in built-up box-type columns. An outline of the program and description of the test methods were presented in Research Paper RP1473.[1]

In this paper are presented the test results for the *C2* series of plates, which were 15 in. wide by ⅜ in. thick, and of which some had ovaloid perforations.

II. COVER-PLATE COLUMNS

1. GENERAL

The details of the *C2* plates and of the angles are shown in figure 1. Each plate shown represents three like plates, designated *(0–1)*, *(2–3)*, and *(4–5)*, and the angle shown represents many like angles which were used interchangeably with the plates to form the columns of which the cross sections are shown in the figure. The composition of the *C2* columns is given in table 1.

TABLE 1.—*Composition of C2 columns*

[The designation of the plate is that of the column minus the item "four angles" or "two angles." The (0–1)-, (2–3)-, and (4–5)-columns whose designations are otherwise the same contained the same angles.]

Column designation	Angle designations
C2A (----) four angles	*C5F(0–1)*, *C5B(2–3)*, *C5M(4–5)*, *C5F(4–5)*.
C2A (----) two angles	*C5F(0–1)*, *C5B(2–3)*.
C2B (----) four angles	*C5F(4–5)*, *C5M(4–5)*, *C5F(2–3)*, *C5G(4–5)*.
C2B (----) two angles	*C5F(4–5)*, *C5M(4–5)*.
C2C (----) four angles	*C5G(4–5)*, *C5F(2–3)*, *C5M(2–3)*, *C5C(4–5)*.
C2C (----) two angles	*C5G(4–5)*, *C5F(2–3)*.
C2D (----) four angles	*C5H(4–5)*, *C5A(4–5)*, *C5B(2–3)*, *C5F(0–1)*.
C2D (----) two angles	*C5H(4–5)*, *C5A(4–5)*.

2. DIMENSIONS

The dimensions given in figure 1 are nominal. There were the usual commercial variations in the thicknesses and widths of the plates and angles. The variations in the dimensions of the perforations were considerably greater; for some plates the difference between the minimum and maximum perforation width was of the order of 0.1 in. The cross-sectional areas of the plates and angles, computed from the measured dimensions, are given in table 2.

[1] Ambrose H. Stang and Martin Greenspan, *Perforated cover plates for steel columns: Program and test methods.* J. Research NBS 28, 669 (1942) RP1473.

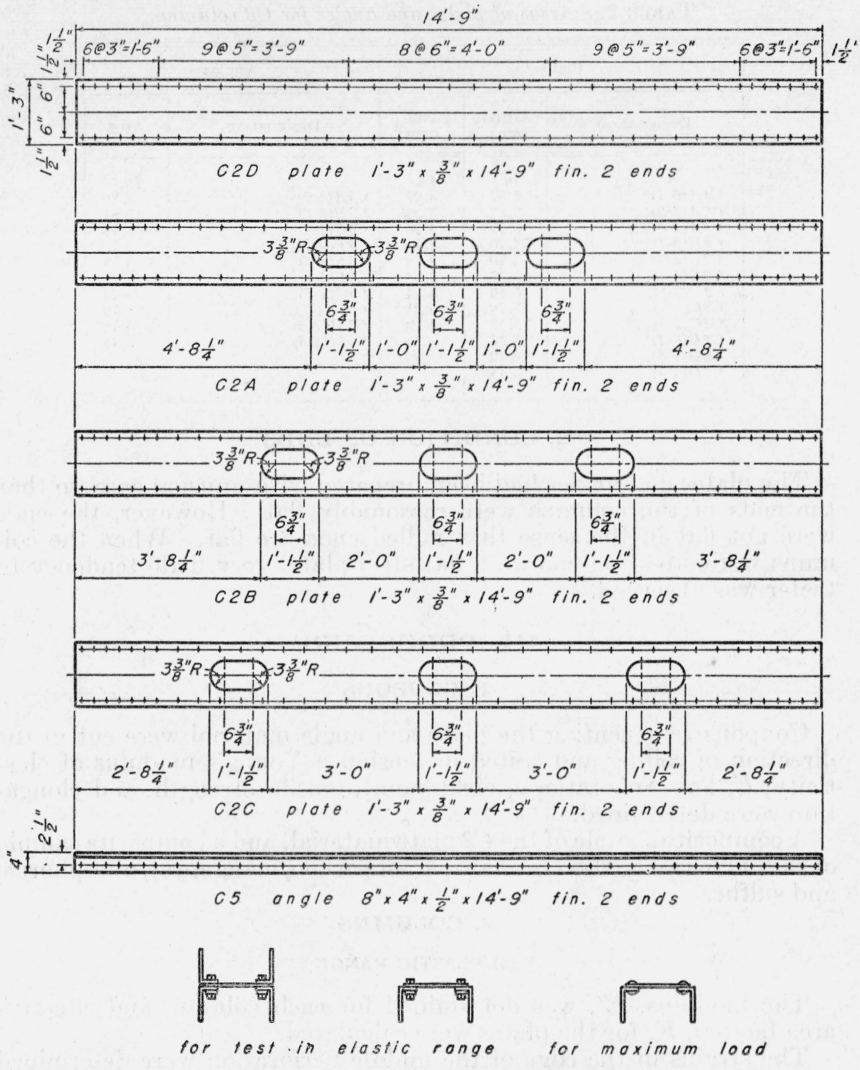

FIGURE 1.—*Plates and angles for the C2 columns.*

TABLE 2.—*Areas of plates and angles for C2 columns*

Plates			Angles	
Designation	Gross area	Net area	Designation	Area
	*in.*²	*in.*²		*in.*²
C2A(0–1)	5.87	3.27	*C5A(4–5)*	5.80
C2A(2–3)	5.82	3.23	*C5B(2–3)*	5.81
C2A(4–5)	5.79	3.23	*C5C(4–5)*	5.75
C2B(0–1)	5.70	3.15	*C5F(0–1)*	5.75
C2B(2–3)	5.70	3.18	*C5F(2–3)*	5.78
C2B(4–5)	5.77	3.19	*C5F(4–5)*	5.75
C2C(0–1)	5.80	3.24	*C5G(4–5)*	5.74
C2C(2–3)	5.76	3.21	*C5H(4–5)*	5.79
C2C(4–5)	5.73	3.19	*C5M(2–3)*	5.71
C2D(0–1)	5.75		*C5M(4–5)*	5.75
C2D(2–3)	5.72			
C2D(4–5)	5.74			

3. CONDITION OF ENDS

The plates and angles had been prepared with unusual care, so that the ends of the columns were reasonably flat. However, the ends were not flat in the sense that milled ends are flat. When the columns were stood on end on a flat steel plate, very little tendency to teeter was observed.

III. PROCEDURE

1. COUPONS

Coupons representing the plate and angle material were cut in the direction of rolling and tested in tension. Young's modulus of elasticity, E, Poisson's ratio, μ, yield point, tensile strength, and elongation were determined.

A composite sample of the *C2* plate material, and a composite sample of the angle material, were analyzed for carbon, manganese, phosphorus, and sulfur.

2. COLUMNS

(a) ELASTIC RANGE

The modulus, E', was determined for each column, and effective area factors, K, for the plates were calculated.

The strains in the edge of the middle perforation were determined for each perforated-plate column. The strains in the surfaces of the plate and in the angles were determined for the middle bay of one of each group of three like perforated-plate columns. The distribution of stress in the middle bay of each of these columns was calculated from the strain data and the values of the elastic constants obtained from the coupon tests.

(b) MAXIMUM LOAD

One two-angle column of each group of three like two-angle columns was subjected to the maximum-load test after the bolts had been replaced by rivets. Data to complete the stress-strain curves and data for the stress-deflection curves were taken. The effective-area factors, C, for the plates, were calculated from the maximum-load values.

IV. RESULTS

1. COUPONS

The results of the tensile tests of the coupons are given in table 3.

TABLE 3.—*Results of tensile tests of coupons*

Coupon designation	Thickness	Young's modulus of elasticity	Poisson's ratio	Yield point	Tensile strength	Elongation in 8 in.
	In.	*Kips/in.²*		*Kips/in.²*	*Kips/in.²*	*Percent*
C2A (1-2)	0.388	29,600	0.283	38.1	58.8	34.0
C2A (3-4)	.387	29,300	.280	37.0	58.4	32.7
C2B (1-2)	.381	29,600	.281	37.7	59.2	34.2
C2B (3-4)	.383	30,000	.284	37.0	59.2	33.8
C2C (1-2)	.386	29,400	.281	37.9	59.8	34.0
C2C (3-4)	.384	29,700	.276	38.4	59.7	33.4
C2D (1-2)	.382	29,600	.288	37.2	58.9	32.9
C2D (3-4)	.381	29,800	.285	37.2	59.0	35.3
C5A (1-2)	.510	29,600	.286	36.3	59.0	33.5
C5A (3-4)	.506	30,000	.290	35.6	58.7	33.5
C5B (1-2)	.506	29,700	.286	36.0	59.5	31.3
C5B (3-4)	.510	29,700	.278	35.9	58.7	35.8
C5C (1-2)	.508	29,400	.281	36.5	58.8	31.3
C5C (3-4)	.501	29,700	.286	34.8	58.3	33.0
C5F (1-2)	.508	29,500	.278	35.4	58.9	32.6
C5F (3-4)	.502	29,200	.277	34.8	59.0	33.6
C5G (1-2)	.509	30,100	.287	37.2	64.3	32.4
C5G (3-4)	.503	29,800	.285	37.0	64.2	31.7
C5H (1-2)	.512	29,400	.279	38.7	65.7	29.0
C5H (3-4)	.506	29,400	.282	38.1	65.7	31.5
C5M (1-2)	.501	29,600	.282	35.3	58.1	31.2
C5M (3-4)	.504	29,100	.270	35.0	58.2	33.6

The chemical composition of the coupon material is given below.

Sample	Carbon	Manganese	Phosphorus	Sulfur
	%	%	%	%
Composite *C2*	0.18	0.58	0.008	0.03
Composite *C5*	.21	.56	.014	.03

2. COLUMNS

(a) MODULUS OF COLUMN AND EFFECTIVE AREA OF PLATE

The moduli, E', of the columns, and the effective-area factors, K, with respect to stiffness, for the plates, are given in table 4.

TABLE 4.—*Moduli of columns, effective-area factors for plates and maximum stresses*

Plate designation	Number of angles	Based on gross area			Based on net area		
		Modulus, E'	Effective-area factor, K	Maximum stress P/A	Modulus, E'	Effective-area factor, K	Maximum stress P/A
		*Kips/in.*²			*Kips/in.*²		
C2A(0-1)	2	25,300	0.60		29,700	1.07	
C2A(2-3)	2	25,500	.62		30,000	1.12	
C2A(4-5)	2	25,600	.62		30,000	1.12	
Avg		25,500	0.61	−2.15	29,900	1.10	−1.83
C2A(0-1)	4	27,100	0.62		29,800	1.11	
C2A(2-3)	4	27,300	.65		30,000	1.17	
C2A(4-5)	4	27,300	.64		29,900	1.15	
Avg		27,200	0.64	−2.03	29,900	1.14	−1.85
C2B(0-1)	2	26,800	0.75		31,500	1.36	
C2B(2-3)	2	26,800	.75		31,400	1.34	
C2B(4-5)	2	27,100	.78		31,900	1.42	
Avg		26,900	0.76	−2.43	31,600	1.37	−2.07
C2B(0-1)	4	27,800	0.72		30,400	1.30	
C2B(2-3)	4	27,700	.71		30,400	1.27	
C2B(4-5)	4	27,800	.73		30,600	1.33	
Avg		27,800	0.72	−2.20	30,500	1.30	−2.01
C2C(0-1)	2	27,200	0.79		31,900	1.42	
C2C(2-3)	2	27,300	.80		32,000	1.43	
C2C(4-5)	2	27,400	.81		32,100	1.45	
Avg		27,300	0.80	−2.52	32,000	1.43	−2.15
C2C(0-1)	4	28,300	0.81		31,000	1.45	
C2C(2-3)	4	28,000	.77		30,700	1.37	
C2C(4-5)	4	28,300	.81		31,000	1.44	
Avg		28,200	0.80	−2.20	30,900	1.42	−2.01
C2D(0-1)	2	29,200			29,200		
C2D(2-3)	2	29,300			29,300		
C2D(4-5)	2	29,200			29,200		
Avg		29,200	1.00		29,200	1.00	
C2D(0-1)	4	29,300			29,300		
C2D(2-3)	4	29,400			29,400		
C2D(4-5)	4	29,400			29,400		
Avg		29,400	1.00		29,400	1.00	

(b) STRESSES

(1) *On the edge of the perforation.*—The distribution of stress on the edge of the middle perforation is shown in figures 2, 3, and 4. Each curve represents the average result for three like columns.

The vertical axis of the graph in each figure is a development of one quadrant of the edge of the perforation. The point B is the point of tangency of the circular and straight parts of the edge.

In the stress ratios $\sigma_{u,v}/(P/A)$, A is the gross area of the column. The stress ratios based on net area, $\sigma_{u,v}/(P/A_n)$, may be obtained by multiplying $\sigma_{u,v}/(P/A)$ by 0.85 for the two-angle, and 0.91 for the four-angle, columns.

The maximum stresses are given in table 4.

(2) *On the surfaces of the plate.*—The distributions of stress on the surfaces of the middle bay for the perforated-plate columns are shown

in figures 5 to 28, inclusive. The stress ratios shown in these figures are based on the gross area. The stress ratios based on the net area may be obtained by multiplying the given values by 0.85 for the two-angle, and 0.91 for the four-angle, columns.

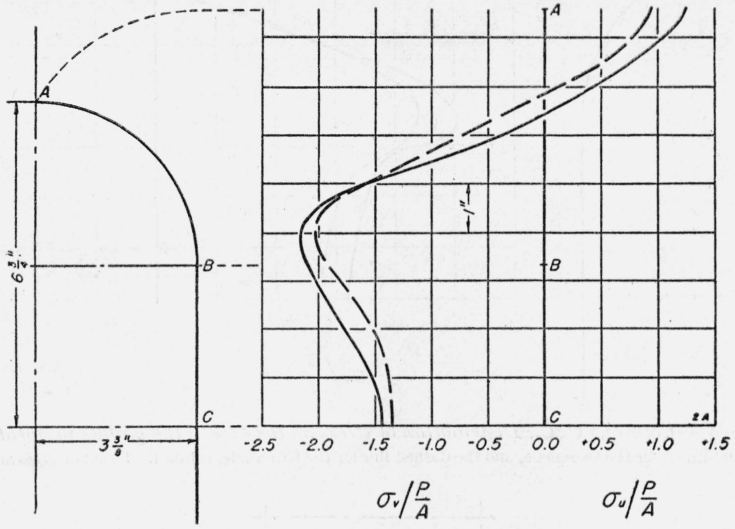

FIGURE 2.—*Columns C2A. Distribution of stress on the edge of the middle perforation.* The solid line is for the two-angle, and the dashed line for the four-angle, column. Based on gross area.

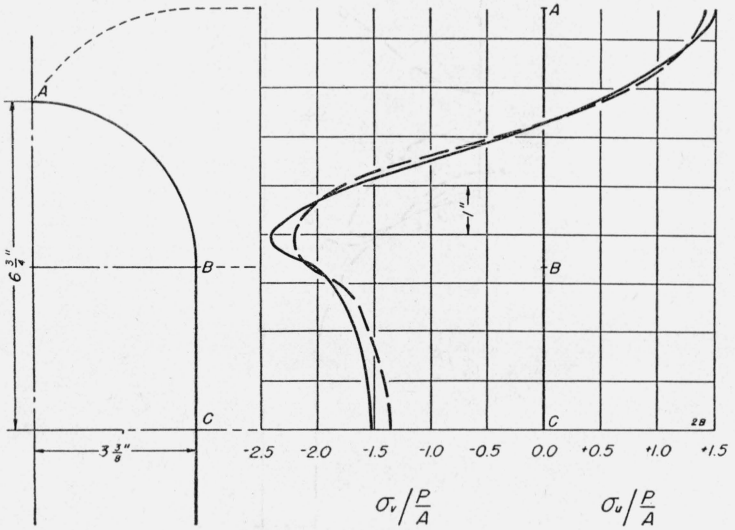

FIGURE 3.—*Columns C2B. Distribution of stress on the edge of the middle perforation.* The solid line is for the two-angle, and the dashed line for the four-angle, column. Based on gross area.

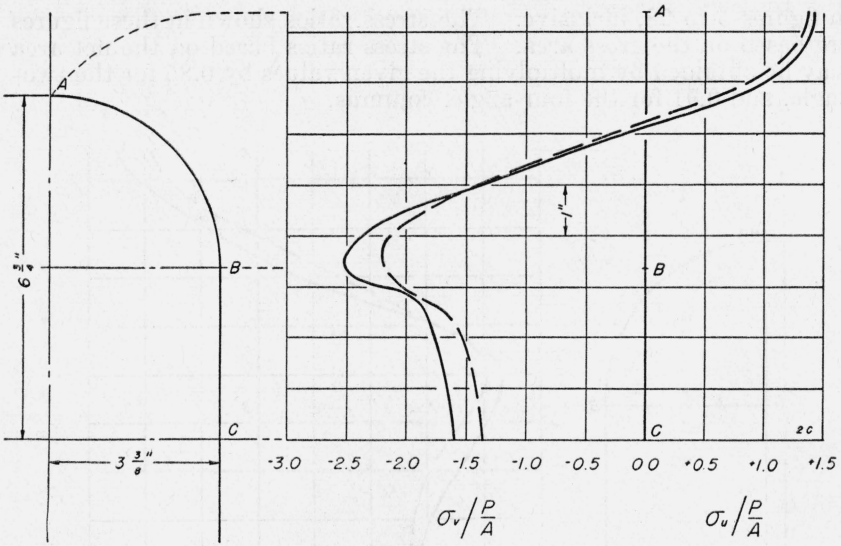

FIGURE 4.—*Columns C2C. Distribution of stress on the edge of the middle perforation.*
The solid line is for the two-angle, and the dashed line for the four-angle, column. Based on gross area.

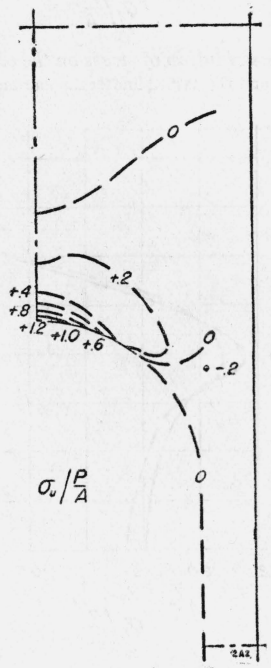

FIGURE 5.—*Column C2A (2–3) (two angles). Isogram of maximum principal stress.*
Based on gross area.

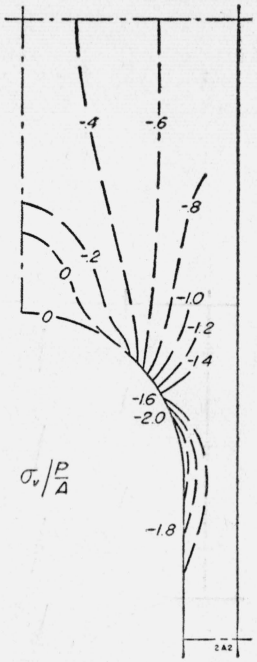

FIGURE 6.—*Column C2A (2–3) (two angles). Isogram of minimum principal stress.*
Based on gross area.

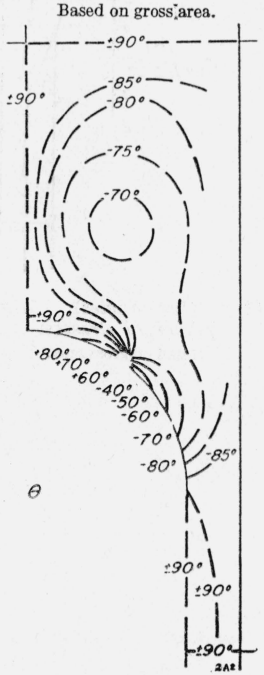

FIGURE 7.—*Column C2A (2–3) (two angles). Isoclinics.*
The angle θ is measured positive counterclockwise from the axis of the column to the direction of σ_n.

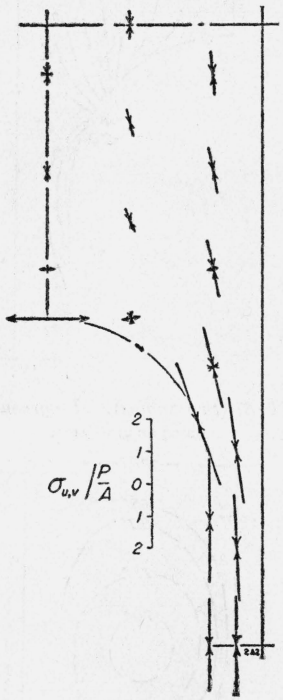

FIGURE 8.—*Column C2A (2–3) (two angles). Magnitude and direction of the principal stresses.*
Based on gross area.

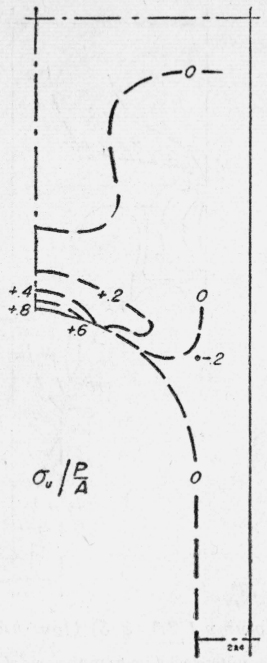

FIGURE 9.—*Column C2A (2–3) (four angles). Isogram of maximum principal stress.*
Based on gross area.

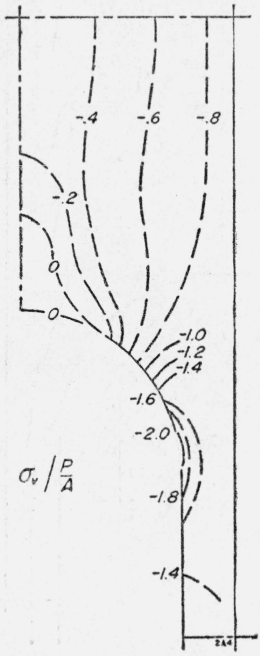

FIGURE 10.—*Column C2A (2–3) (four angles). Isogram of minimum principal stress.*
Based on gross area.

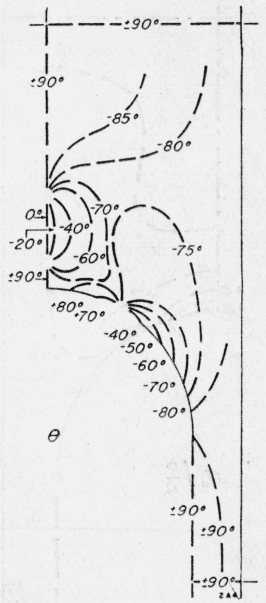

FIGURE 11.—*Column C2A (2–3) (four angles). Isoclinics.*

The angle θ is measured positive counterclockwise from the axis of the column to the direction of σ_1.

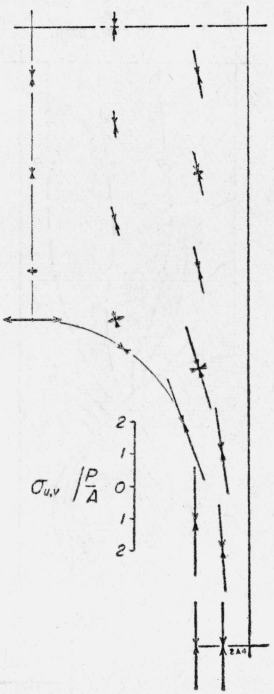

FIGURE 12.—*Column C2A (2–3) (four angles). Magnitude and direction of the principal stresses.*

Based on gross area.

FIGURE 13.—*Column C2B (2–3) (two angles). Isogram of maximum principal stress.*
Based on gross area.

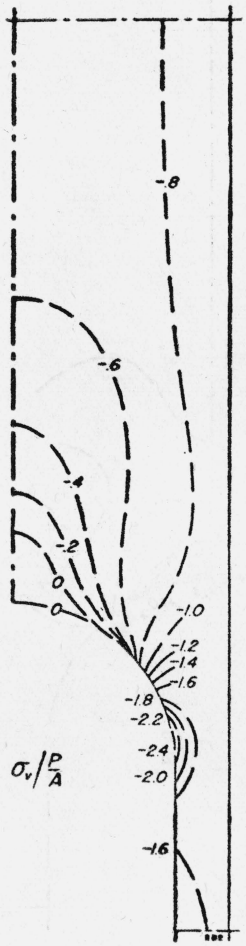

FIGURE 14.—*Column C2B (2–3) (two angles). Isogram of minimum principal stress.*

Based on gross area.

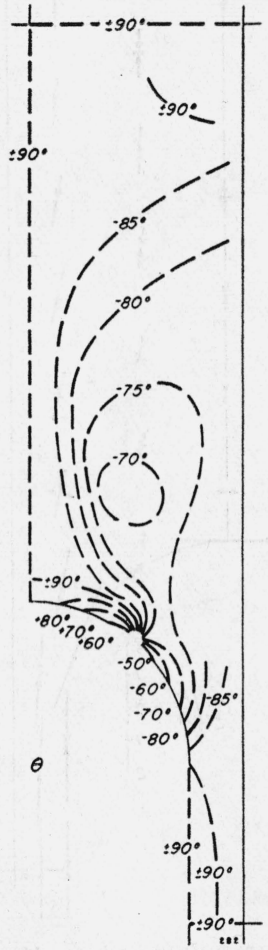

FIGURE 15.—*Column C2B (2–3) (two angles). Isoclinics.*

The angle θ is measured positive counterclockwise from the axis of the column to the direction of σ_2.

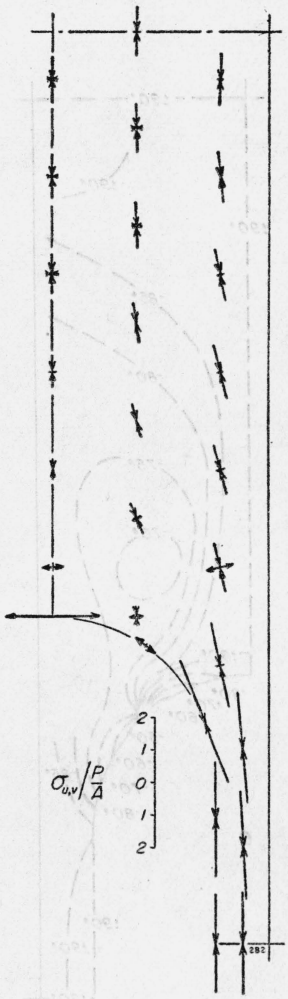

FIGURE 16.—*Column C2B (2–3) (two angles). Magnitude and direction of the principal stresses.*
Based on gross area.

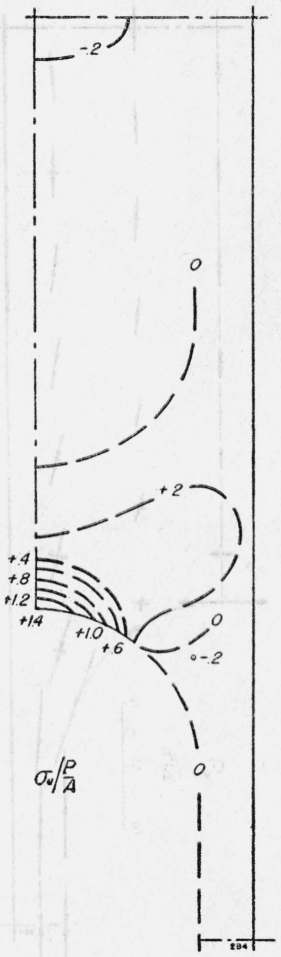

FIGURE 17.—*Column C2B (2–3) (four angles). Isogram of maximum principal stress.*
Based on gross area.

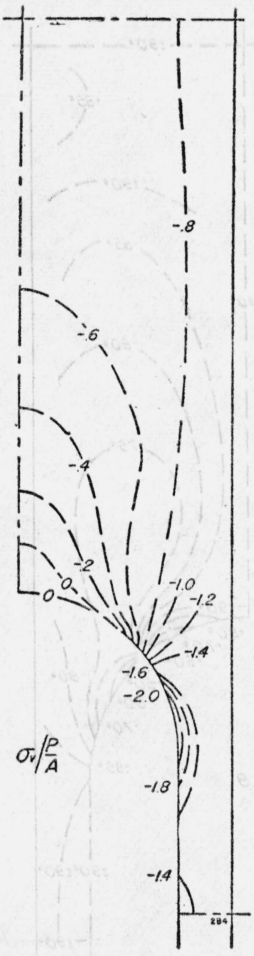

FIGURE 18.—*Column C2B (2–3) (four angles). Isogram of minimum principal stress.*
Based on gross area.

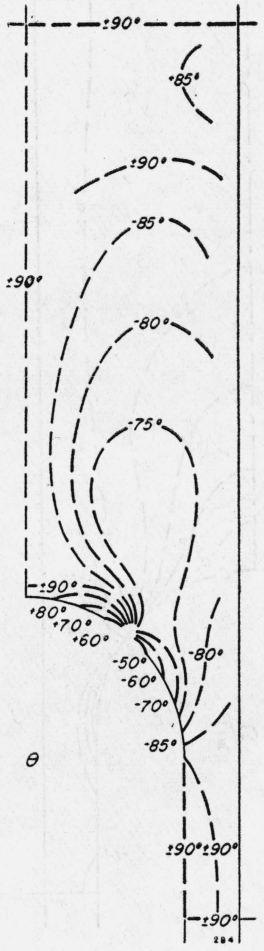

FIGURE 19.—*Column C2B (2–3) (four angles). Isoclinics.*

The angle θ is measured positive counterclockwise from the axis of the column to the direction of σ_u.

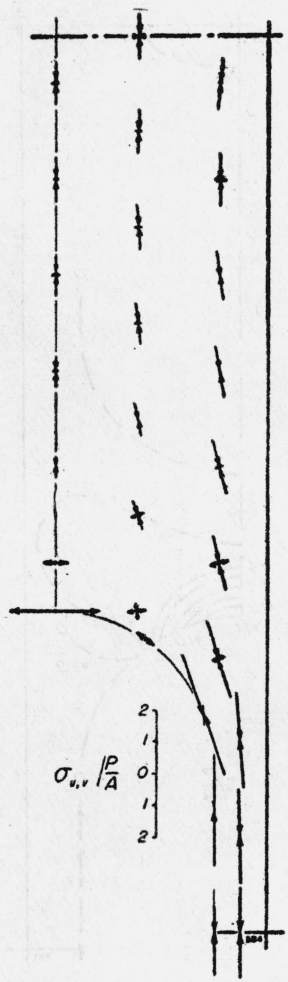

FIGURE 20.—*Column C2B (2–3) (four angles). Magnitude and direction of the principal stresses.*

Based on gross area.

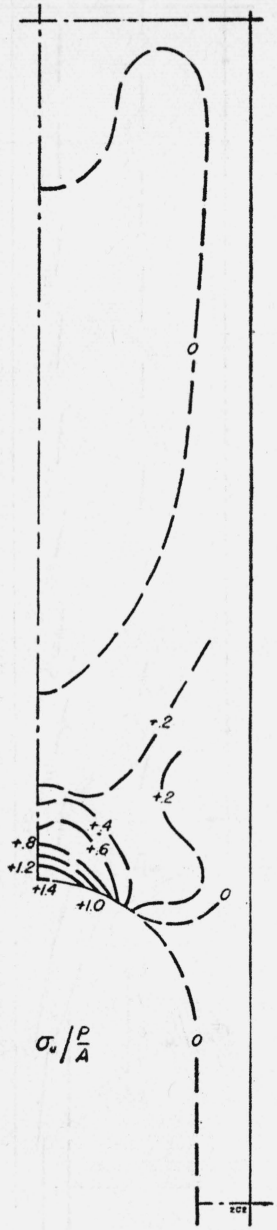

FIGURE 21.—*Column C2C (2–3) (two angles). Isogram of maximum principal stress.*
Based on gross area

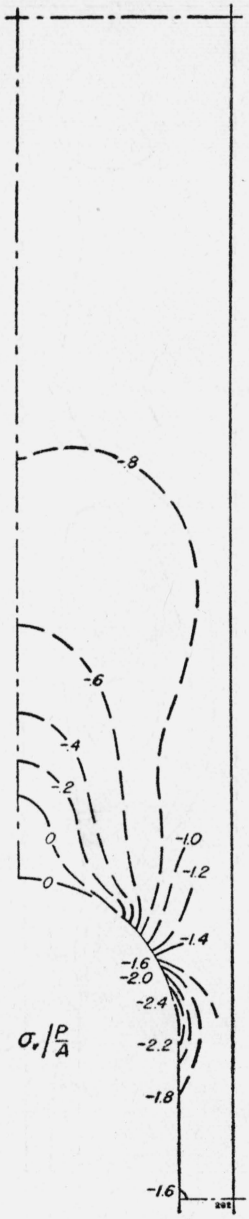

FIGURE 22.—*Column C2C (2–3) (two angles). Isogram of minimum principal stress.*
Based on gross area.

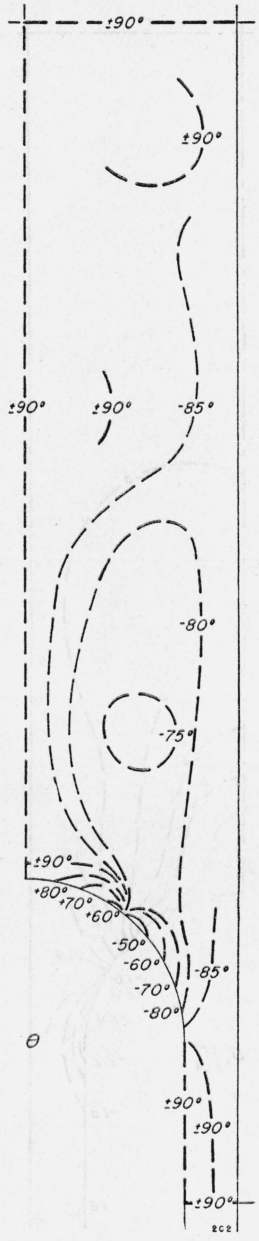

FIGURE 23.—*Column C2C (2–3) (two angles). Isoclinics.*

The angle θ is measured positive counterclockwise from the axis of the column to the direction of σ_u.

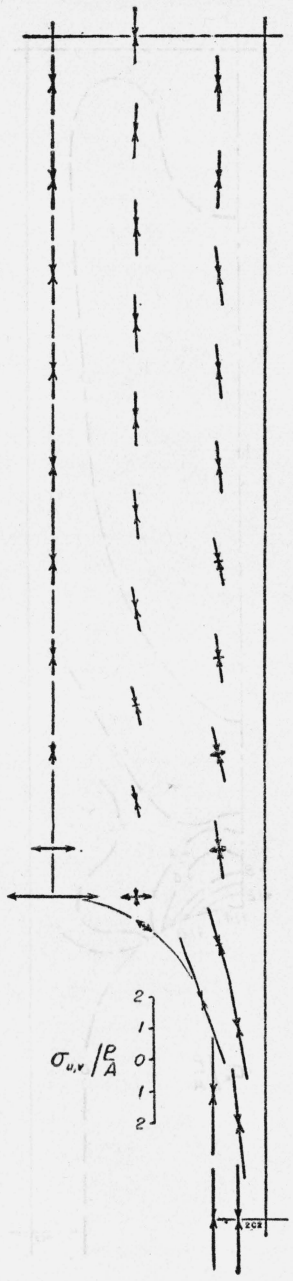

FIGURE 24.—*Column C2C (2–3) (two angles). Magnitude and direction of the principal stresses.*

Based on gross area.

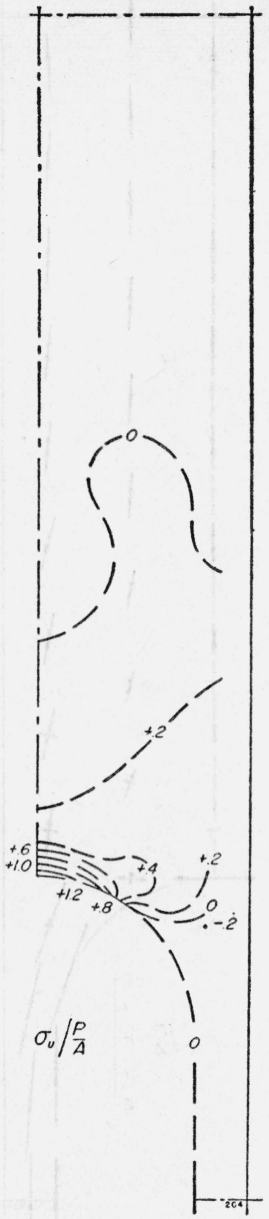

FIGURE 25.—*Column C2C (2–3) (four angles). Isogram of maximum principal stress.*

Based on gross area.

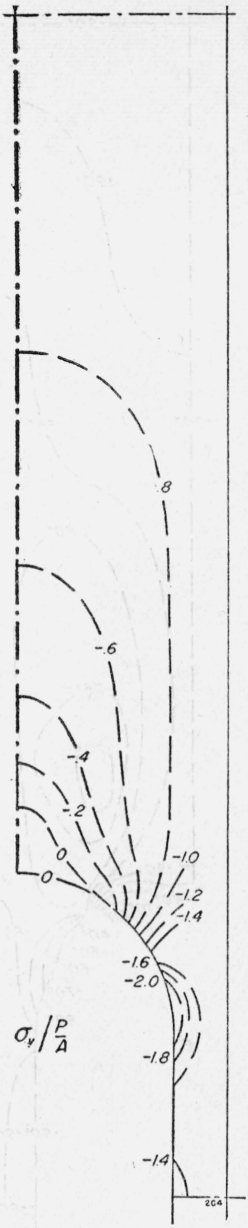

FIGURE 26.—*Column C2C (2–3) (four angles). Isogram of minimum principal stress.*

Based on gross area.

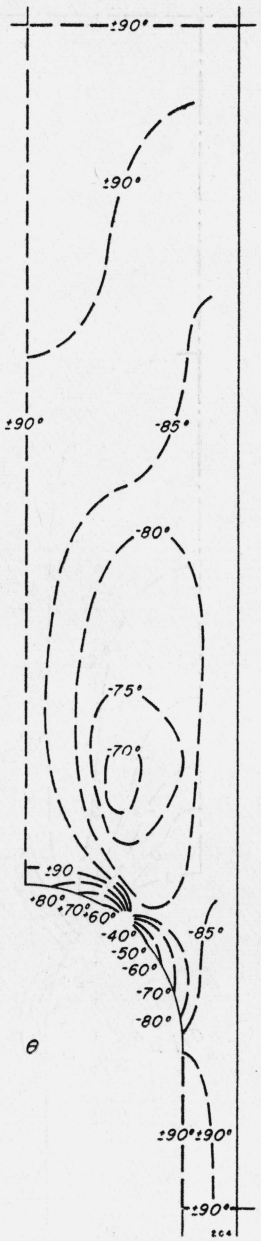

FIGURE 27.—*Column C2C (2–3) (four angles). Isoclinics.*

The angle θ is measured positive counterclockwise from the axis of the column to the direction of σ_3.

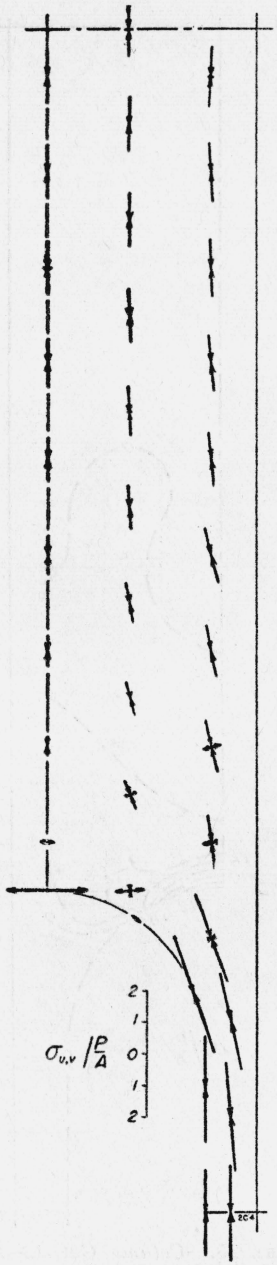

FIGURE 28.—*Column C2C (2–3) (four angles). Magnitude and direction of the principal stresses.*

Based on gross area.

The effect of the perforation on the stress distribution may be judged from the fact that for a solid plate (no perforation) the values everywhere of $\sigma_u/(P/A)$ are zero; of $\sigma_v/(P/A)$, -1; and of θ, 90 degrees.

(3) *On the angles.*—The variation of stress along the length of the angles is shown for column *C2B(2–3)* (two angles) in figure 29. The point *D* is at midlength of the perforation, the point *E* midway between perforations. As the stresses at the various points differed from one another by amounts of the order of magnitude of the experimental error of measurement, the stress was substantially constant along the length of the angles. Similar results were obtained for the remainder of the columns, except that for the *C2A* columns, there was some tendency for the stress in the angles to decrease near the perforation, as might be expected from the theory for a circular hole in a plate of finite width.

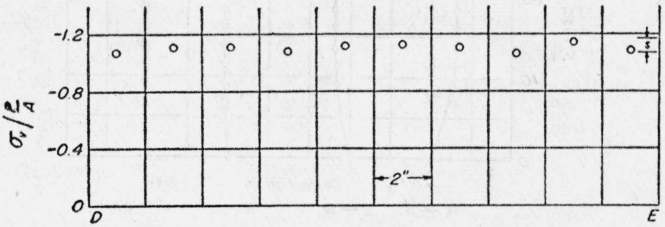

FIGURE 29.—*Column C2B (2–3) (two angles). Variation of stress along the length of the angles.*

Based on gross area. The circles represent stresses calculated from the observed strains. The stress-interval, *S*, corresponds to one division on the dial of the strain gage.

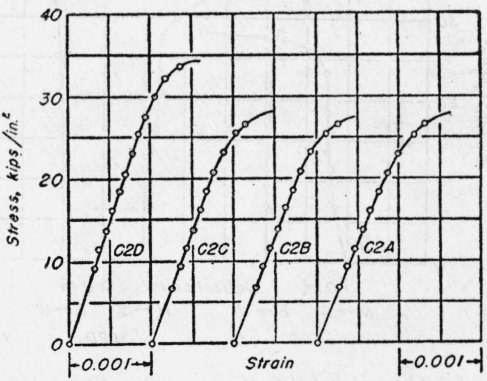

FIGURE 30.—*Columns C2–(2–3) (two angles). Stress-strain graphs.*

Based on gross area.

The stress ratios on a net-area basis may be obtained by multiplying those shown by the factor 0.85.

(c) MAXIMUM-LOAD TEST

(1) *Stress-strain graphs.*—The stress-strain graphs for the columns are shown in figure 30.

The stresses on the net area may be obtained by multiplying the stresses on the gross area by 1.17.

(2) *Deflections.*—The stress-lateral-deflection graphs for the columns are shown in figure 31.

The stresses on the net area may be obtained by multiplying the stresses on the gross area by 1.17.

(3) *Maximum load and effective area of plate.*—The maximum loads for the columns, the maximum average stress on the gross area and on the net area, and the effective-area factors of the plates with respect to compressive strength, C, are given in table 5.

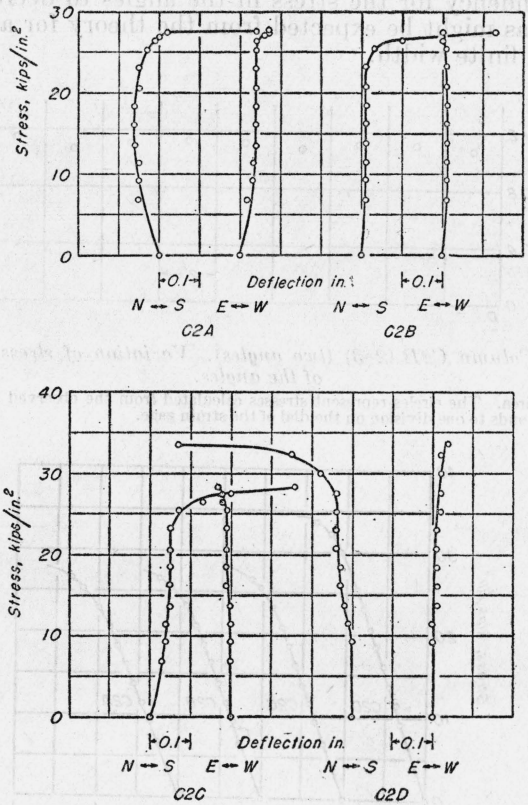

FIGURE 31.—*Columns C2–(2–3) (two angles). Stress-deflection graphs.*
Based on gross area. When the deflection is north, N, the bending stress is tensile on the plate side.

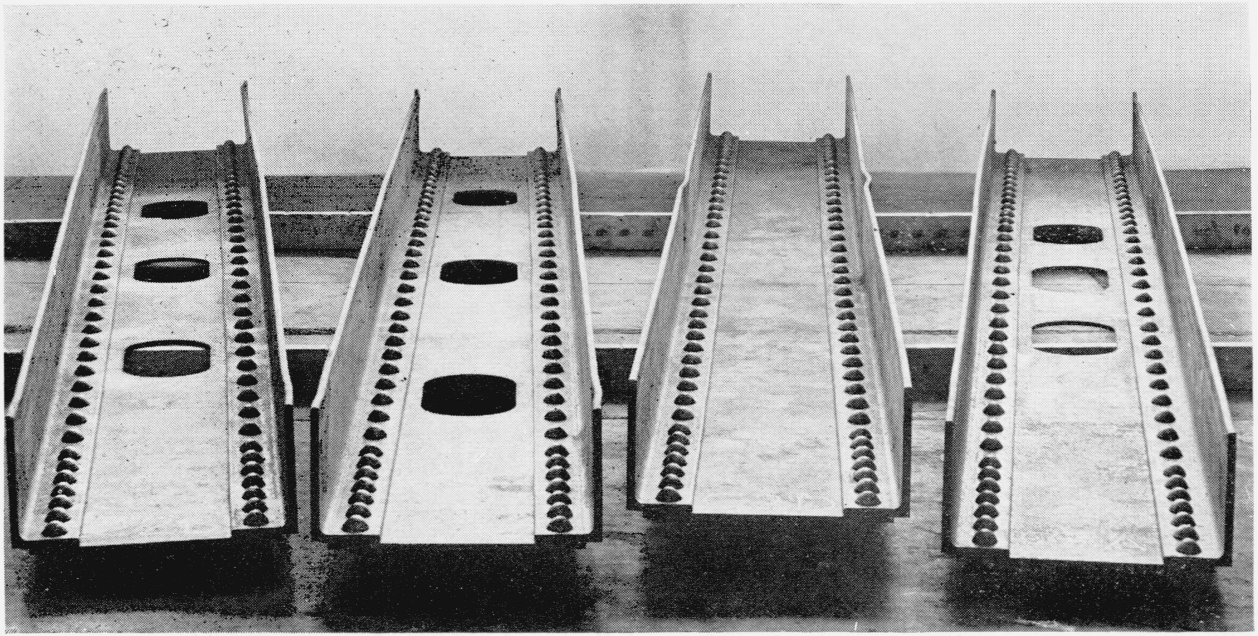

FIGURE 32.—*Columns C2–(2–3) (two angles) after maximum-load tests.*

From left to right, the columns are *C2B, C2C, C2D,* and *C2A,* respectively.

TABLE 5.—*Maximum loads for columns and effective-area factors for plates*

Column designation	*C2A*	*C2B*	*C2C*	*C2D*
Perforation spacing, in.	25.5	37.5	49.5	[a]
Area of angles, in.²	11.55	11.50	11.52	11.59
Gross area of plate, in.²	5.82	5.70	5.76	5.72
Net area of plate, in.²	3.23	3.18	3.21	5.72
Total area, gross, in.²	17.37	17.20	17.28	17.31
Total area, net, in.²	14.78	14.68	14.73	17.31
Maximum compressive load, kips	483	473	490	585
Compressive stress on gross area at failure, kips/in.²	27.8	27.5	28.4	33.8
Compressive stress on net area at failure, kips/in.²	32.7	32.3	33.3	33.8
Effective-area factor of plate with respect to compressive strength, *C*:				
Based on gross area	0.47	0.44	0.52	1.00
Based on net area	.85	.79	.93	
Slenderness ratio				70
Column efficiency, percent				91

[a] No perforations.

All four columns failed by primary buckling.

The perforated-plate columns, *C2A*, *C2B*, and *C2C*, failed away from the plate side (toward the south) of the column, as would be expected from the consideration that, in the neighborhood of a perforation, the gravity axis of the column is displaced away from the plate side. Local buckling of the outstanding legs of the angles of the columns occurred near the ends of the columns.

The unperforated-plate column, *C2D*, failed toward the plate side, as would be expected from the double-modulus column theory. The column efficiency of 91 percent, given in table 5, is the ratio of the average compressive stress at failure to the weighted average yield point of the material determined from the tensile tests of the coupons.

Figure 32 shows the columns after test.

V. SUMMARY

1. MODULUS

The effectiveness of the perforated plates in resisting shortening under compressive load was determined by comparison of the modulus of a column containing the perforated plate with that of a similar column containing an unperforated plate. It was found that from 60 to 80 percent of the cross-sectional area of the plate, depending on the perforation spacing, was effective. The effective-area factors for the perforated plates were not consistently affected by variation in the number of angles with which they were tested.

2. STRESS DISTRIBUTION

The stress distribution was determined on the middle bay of one of each group of three like columns. In every case the maximum stress was compressive and occurred on the edge of the perforation. The value of the maximum stress was only slightly affected by variation of the perforation spacing. For columns with the same perforation spacing, the maximum stress was higher for the two-angle than for the four-angle column for the same average stress on the gross area. This was not always true when the stresses were based on the net area.

The maximum stress varied from 2 to 2.5 times the average stress on the gross area, or 1.8 to 2.1 times the average stress on the net area.

The presence of the perforations did not materially affect the stresses in the angles.

3. STRENGTH

The effectiveness of the perforated plates with respect to strength was lower than with respect to resistance to shortening, and was practically independent of the perforation spacing.

WASHINGTON, February 28, 1942.